Structure and Molecular Ordering of a Nematic Liquid Crystal Studied by Natural-Abundance Double-Quantum ^{13}C NMR

D. Sandström* and M. H. Levitt

Contribution from the Division of Physical Chemistry, Arrhenius Laboratory, Stockholm University, S-106 91 Stockholm, Sweden

Received January 19, 1996[⊗]

Abstract: We have studied the mesogenic molecule 4-*n*-pentyl-4′-cyanobiphenyl (5CB) in the nematic phase by double-quantum ^{13}C nuclear magnetic resonance (NMR). The experiment detects selectively the very rare isotopomers containing natural pairs of ^{13}C spins. The $^{13}C-^{13}C$ dipolar couplings were interpreted in terms of the structure and orientational order of the cyanobiphenyl fragment. Different strategies were employed to analyze the internal motion of the core moiety. This is the first investigation of molecular conformation and order which exploits magnetic $^{13}C-^{13}C$ dipolar couplings in a non-labeled liquid crystal.

1. Introduction

Liquid crystals are characterized by long-range orientational order combined with high translational molecular mobility. Such mesophases are often exhibited by rod-like molecules with a substantial degree of internal flexibility. Understanding of the liquid crystalline phase requires knowledge of how the molecular orientation couples with the internal conformational degrees of freedom. Nuclear magnetic resonance (NMR) spectroscopy is an important experimental tool for liquid crystalline investigations since it can give detailed information about molecular geometry, average orientation, and internal dynamics.

Deuterium NMR is a popular choice due to the simple and intense spectra,[1] but it has some disadvantages. First, site-specific isotopic labeling is usually required. This can be both difficult and expensive. Second, high-field ^{2}H NMR spectra are dominated by the interaction of the electric quadrupole moment of the nucleus with the surrounding electric field gradients. Dipole−dipole couplings are weak and difficult to observe. As a result, the ^{2}H spectra depend strongly on molecular orientation but are rather insensitive to details of molecular conformation. Third, interpretation of the results requires estimation of the magnitude of the electric field gradient (EFG) at the deuterium site. Usually it must be assumed that the EFG is not significantly conformation-dependent.

NMR of spin-$^1/_2$ nuclei is potentially more informative since the spectra depend strongly on through-space magnetic dipole−dipole (DD) interactions. These interactions are sensitive both to spin−spin distances and to angles between the external field and the internuclear vectors. However, it is difficult to extract the individual DD couplings from proton NMR, since the spectra are extremely complicated except for very small molecules. The spectra may be greatly simplified by exploiting high orders of multiple-quantum coherence.[2] However, each line frequency still depends on a large number of dipolar couplings, so extraction of the individual DD couplings remains problematic.

The number of coupled protons may be reduced by means of either selective[3] or random[4] deuteration. This simplifies the spectral analysis somewhat, but requires preparation of isotopically substituted compounds and leaves problems of peak assignment and deuteron decoupling. Another approach has been to record proton−carbon dipolar couplings,[5] but this requires multipulse sequences to average out the proton−proton interactions. These complicated schemes are associated with pulse imperfections, sensitivity, and heating problems. Furthermore, the observed DD couplings are reduced by a sequence-dependent scaling factor which must be calibrated. Only short-range heteronuclear dipolar couplings have been estimated this way.

In nematic phases, ^{1}H-decoupled ^{13}C spectra are quite easy to obtain but have generally been regarded as rather uninformative. Since the natural abundance of ^{13}C is low (≈1%), the spectra do not display any obvious dipole−dipole couplings. The line positions are determined by the isotropic ^{13}C chemical shifts and motional averages of the ^{13}C chemical shift anisotropies. In principle, information about orientational ordering may be obtained, but this requires knowledge of the orientation of the chemical shift tensors in some molecular-fixed axis system.[6] As a result, ^{1}H-decoupled ^{13}C NMR spectroscopy of liquid crystals has been relatively neglected.

Recently, we demonstrated that useful spectral structure lies buried below the dominant signals in an ordinary ^{13}C spectrum of a nematic mesophase.[7] Borrowing ideas from double-quantum ^{13}C spectroscopy of isotropic liquids,[8,9] we used the special phase properties of double-quantum coherence (2QC) to filter out the signals from molecules containing pairs of ^{13}C spins. Such signals are extremely weak since a given pair of carbon sites is only occupied by two ^{13}C spins in around 0.02% of the molecules in the sample. However, the spectral contributions from such minor isotopomers are very informative since (i) they are sensitive to the dipolar coupling between the spin-pairs, (ii) the spectra are easy to analyze since only two spins are involved if the abundant ^{1}H spins are decoupled, and (iii) the contributions from the large number of different ^{13}C isotopomers are easily separated by utilizing the double-quantum

* Address correspondence to this author (dick@physc.su.se).

[⊗] Abstract published in *Advance ACS Abstracts,* June 15, 1996.

(1) Goldfarb, D.; Poupko, R.; Luz, Z.; Zimmermann, H. *J. Chem. Phys.* **1983**, *79*, 4035−4047.
(2) Sinton, S.; Pines, A. *Chem. Phys. Lett.* **1980**, *76*, 263−267.
(3) Emsley, J. W.; Horne, T. J.; Zimmermann, H.; Celebre, G.; Longeri, M. *Liq. Cryst.* **1990**, *7*, 1−13.
(4) Gochin, M.; Schenker, K. V.; Zimmermann, H.; Pines, A. *J. Am. Chem. Soc.* **1986**, *108*, 6813−6814.
(5) Fung, B. M.; Afzal, J. *J. Am. Chem. Soc.* **1986**, *108*, 1107−1108.
(6) Pines, A.; Chang, J. J. *J. Am. Chem. Soc.* **1974**, *96*, 5590−5591.
(7) Sandström, D.; Summanen, K. T.; Levitt, M. H. *J. Am. Chem. Soc.* **1994**, *116*, 9357−9358.
(8) Bax, A.; Freeman, R.; Kempsell, S. P. *J. Am. Chem. Soc.* **1980**, *102*, 4849−4851.
(9) Bax, A.; Freeman, R.; Frenkiel, T. A.; Levitt, M. H. *J. Magn. Reson.* **1981**, *43*, 478−483.

S0002-7863(96)00185-0 CCC: $12.00

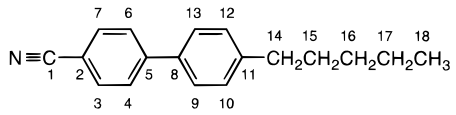

Figure 1. Chemical structure of 4-*n*-pentyl-4′-cyanobiphenyl (5CB) showing the carbon labeling.

precession frequency, which is the sum of the chemical shift frequencies of the two coupled spins. In many cases, the two involved ^{13}C spins may be assigned by inspection.

The main disadvantage of the double-quantum ^{13}C technique is its very low sensitivity when performed on natural material. Similar experiments have previously been employed to extract $^{13}C-^{13}C$ dipolar splittings from molecules oriented in phospholipid bilayers.[10] There, however, isotopically labeled compounds were used.

In this article we study the nematic liquid crystal formed by the rod-like molecule 4-*n*-pentyl-4′-cyanobiphenyl (5CB) with the phase director oriented spontaneously along the magnetic field of the spectrometer. We chose this system because (i) it has been extensively investigated by other methods[2,11−17] and (ii) the conformation of the biphenyl fragment is described by a single parameter, the torsional angle, allowing a relatively simple analysis. We did not attempt to study the dynamics and conformation of the mobile aliphatic chain, for reasons mentioned below. We used two different approaches to analyze the $^{13}C-^{13}C$ dipolar couplings within the core: (i) a simple analysis in terms of the orientational order parameters of the two individual rings, and (ii) a more sophisticated approach taking into account the torsional angle distribution and its influence on the orientational order of the biphenyl fragment.

2. Double-Quantum ^{13}C NMR in Ordered Media

In this section we review the relevant aspects of the theory of two-spin systems and double-quantum spectroscopy in ordered media.

2.1. Spin Hamiltonian. The rotating-frame spin Hamiltonian for two coupled ^{13}C spins S_j and S_k in high magnetic field may be written

$$H = H_j + H_k + H_{jk} \tag{1}$$

where H_j is the chemically-shifted Zeeman interaction of spin S_j in the rotating reference frame

$$H_j = \omega_j^0 S_{jz} \tag{2}$$

where

$$\omega_j^0 = \omega_{0S}\langle 1 - \sigma_j\rangle - \omega^{\mathrm{RF}} \tag{3}$$

and similarly for H_k. Here $\omega_{0S} = -\gamma_S B_0$ is the Larmor frequency, γ_S is the magnetogyric ratio, and σ_j is the orientation-dependent shielding constant for spins at site j. The angular brackets $\langle ...\rangle$ denote an average over the rapid anisotropic motion of the molecules in the ordered phase, and ω^{RF} is the frequency of the rotating reference frame, equal in sign and similar in magnitude to the Larmor frequency ω_{0S}. For spins with positive magnetogyric ratio γ, $\omega^{\mathrm{RF}} = -\omega^{\mathrm{carrier}}$, where $\omega^{\mathrm{carrier}}$ is the spectrometer reference frequency. With this consistent treatment of signs, conventionally-presented spectra are labeled with negative rotating-frame frequencies on the left and positive rotating-frame frequencies on the right (in the case of $\gamma > 0$).[18] It is particularly important to be consistent about signs when different classes of interactions are mixed, as is the case here.

Table 1. Eigenstates and Eigenvalues of the Rotating-Frame Hamiltonian of a Two-Spin System

eigenstate	eigenvalue
$\|1\rangle = \|\alpha\alpha\rangle$	$^1/_2(\omega_\Sigma + \omega_A)$
$\|2\rangle = \cos\theta\|\alpha\beta\rangle + \sin\theta\|\beta\alpha\rangle$	$^1/_2(\omega_e - \omega_A)$
$\|3\rangle = -\sin\theta\|\alpha\beta\rangle + \cos\theta\|\beta\alpha\rangle$	$^1/_2(-\omega_e - \omega_A)$
$\|4\rangle = \|\beta\beta\rangle$	$^1/_2(-\omega_\Sigma + \omega_A)$

The spin−spin coupling is given by

$$H_{jk} = H_{jk}^{(0)} + H_{jk}^{(2)} \tag{4}$$

where the isotropic (rank 0) and anisotropic (rank 2) parts are

$$H_{jk}^{(0)} = 2\pi J_{jk}^{\mathrm{iso}} \mathbf{S}_j \cdot \mathbf{S}_k \tag{5}$$

and

$$H_{jk}^{(2)} = D_{jk}(3S_{jz}S_{kz} - \mathbf{S}_j \cdot \mathbf{S}_k) \tag{6}$$

The Hamiltonian terms $H_{jk}^{(L)}$ are secular components of irreducible spherical tensors, transforming as rank L under spatial rotations of the molecular framework, holding the magnetic field and spin polarizations fixed. The second-rank part of the dipole−dipole coupling has contributions from the through-space spin−spin interaction as well as from the anisotropy of the electron-mediated J-coupling:

$$D_{jk} = -\frac{\mu_0}{4\pi}\gamma_S^2\hbar\left\langle\frac{1}{2}(3\cos^2\theta_{jk} - 1)r_{jk}^{-3}\right\rangle + 2\pi\langle J_{jk}^{\mathrm{aniso}}\rangle \tag{7}$$

r_{jk} is the spin-spin distance and θ_{jk} is the angle between the spin-spin vector and the magnetic field. It is not possible to distinguish experimentally between the through-space part of the DD coupling and the J-anisotropy contribution.

The well-known eigenvalues and eigenvectors (eigenstates) are given in Table 1, which uses the following definitions:

$$\omega_\Sigma = \omega_j^0 + \omega_k^0 \tag{8}$$

$$\omega_\Delta = \omega_j^0 - \omega_k^0 \tag{9}$$

$$\omega_A = \pi J_{jk}^{\mathrm{iso}} + D_{jk} \tag{10}$$

$$\omega_B = 2\pi J_{jk}^{\mathrm{iso}} - D_{jk} \tag{11}$$

$$\omega_e = (\omega_\Delta^2 + \omega_B^2)^{1/2} \tag{12}$$

$$\tan 2\theta = \omega_B/\omega_\Delta \tag{13}$$

The conventional one-dimensional spectrum of the AB system contains four lines, each associated with one of the four (−1)-

(10) Sanders, C. R.; Prestegard, J. H. *J. Am. Chem. Soc.* **1991**, *113*, 1987−1996.
(11) Emsley, J. W.; Luckhurst, G. R.; Gray, G. W.; Mosley, A. *Mol. Phys.* **1978**, *35*, 1499−1503.
(12) Emsley, J. W.; Luckhurst, G. R.; Stockley, C. P. *Mol. Phys.* **1981**, *44*, 565−580.
(13) Sinton, S. W.; Zax, D. B.; Murdoch, J. B.; Pines, A. *Mol. Phys.* **1984**, *53*, 333−362.
(14) Fung, B. M.; Afzal, J.; Foss, T. L.; Chau, M. H. *J. Chem. Phys.* **1986**, *85*, 4808−4814.
(15) Frech, C. B.; Fung, B. M.; Schadt, M. *Liq. Cryst. Chem. Phys. Appl.* **1989**, *1080*, 215−226.
(16) Celebre, G.; Longeri, M.; Sicilia, E.; Emsley, J. W. *Liq. Cryst.* **1990**, *7*, 731−737.
(17) Catalano, D.; Di Bari, L.; Veracini, C. A.; Shilstone, G. N.; Zannoni, C. *J. Chem. Phys.* **1991**, *94*, 3928−3935.
(18) Levitt, M. H. To be submitted for publication.

Table 2. Spectral Frequencies and Amplitudes in One-Pulse 1D NMR Spectroscopy of an Ensemble of Two-Spin Systems

coherence state pair	freq ω_{rs}	amplitude a_{rs}
$\|4\rangle\langle 3\|$	$^1/_2(\omega_\Sigma - \omega_e - 2\omega_A)$	$1 - \sin 2\theta$
$\|2\rangle\langle 1\|$	$^1/_2(\omega_\Sigma - \omega_e + 2\omega_A)$	$1 + \sin 2\theta$
$\|4\rangle\langle 2\|$	$^1/_2(\omega_\Sigma + \omega_e - 2\omega_A)$	$1 + \sin 2\theta$
$\|3\rangle\langle 1\|$	$^1/_2(\omega_\Sigma + \omega_e + 2\omega_A)$	$1 - \sin 2\theta$

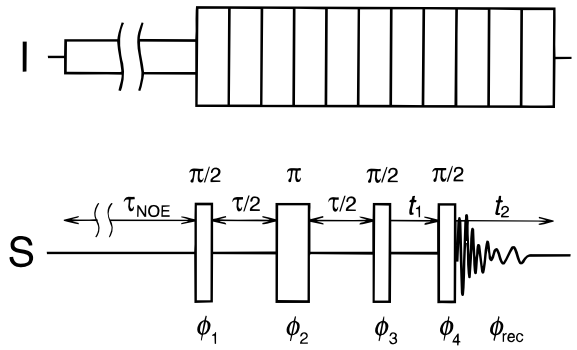

Figure 2. Pulse sequence for the 2D double-quantum NMR experiment. The modulated proton decoupling and the phase cycling of the rf pulses in the carbon channel are described in the text.

quantum operators $|2\rangle\langle 1|$, $|3\rangle\langle 1|$, $|4\rangle\langle 2|$, and $|4\rangle\langle 3|$. The frequency ω_{rs} of the peak associated with the state pair $|r\rangle\langle s|$ is

$$\omega_{rs} = -\omega_r + \omega_s \tag{14}$$

The amplitudes a_{rs} of the spectral peaks depend on the pulse sequence: For simple one-pulse excitation, the amplitudes are proportional to

$$a_{rs} = |\langle r|S_{j-} + S_{k-}|s\rangle|^2 \tag{15}$$

The frequencies and amplitudes of the signals generated by the four observable (−1)-quantum coherences are, in the case of simple one-pulse excitation, given in Table 2. If the dipolar coupling D_{jk} is larger than the isotropic J-coupling, the result is a characteristic pattern in which the outer lines are stronger than the inner lines.

2.2. Two-Dimensional Double-Quantum Spectroscopy. Two-dimensional (2D) double-quantum spectra of the ^{13}C spin-pairs are obtained with the standard pulse sequence shown in Figure 2. The pulse scheme starts with an extended period of irradiation at the ^{1}H Larmor frequency to enhance the longitudinal ^{13}C magnetization by the steady-state nuclear Overhauser effect.[19] A three-pulse sequence over duration τ is applied to the ^{13}C spins to excite (±2)Q coherences $|1\rangle\langle 4|$ and $|4\rangle\langle 1|$ within the dilute spin-pairs. The (±2)Q coherences evolve at the rotating-frame frequency $\mp\omega_\Sigma$ during the variable evolution period t_1 and are reconverted into detectable (−1)Q coherences by the final $\pi/2$ pulse, which are observed during the detection period t_2. Modulated ^{1}H decoupling is applied throughout (see below). A 2D signal matrix $s(t_1,t_2)$ is built up by repeating the experiment for many different values of t_1. Double Fourier transformation gives a spectrum in which each set of spin-pair signals is distinguished by the characteristic frequency coordinate ω_Σ of the peaks in the ω_1 dimension.

Extensive phase cycling is used to suppress signals from isolated ^{13}C spins which cannot support (±2)Q coherence (see Experimental Section). Pure absorption phase 2D spectra are produced by combining together (+2)- and (−2)-quantum signals in a standard procedure.[20] It is not obvious that the (±2)-quantum signals have the correct amplitude balance in a strongly-coupled AB system to make the pure absorption phase possible. The theoretical treatment in ref 21 did not resolve this issue. In the Appendix, it is shown that if the last pulse has a flip angle of $\pi/2$, the coherence transfer amplitudes do have the required symmetries for pure absorption phase. The relative amplitudes of the spectral lines are exactly the same as in a conventional 1D spectrum, except for a sign change of two out of the four lines and relaxation losses. The frequency coordinates and amplitudes of the 2D spectral peaks are given in Table 3. The double-quantum excitation factor $g(\tau)$ was calculated by Nakai et al.[22] and is given by

$$g(\tau) = \left[\left(\frac{\omega_\Delta}{\omega_e}\right)^2 + \left(\frac{\omega_B}{\omega_e}\right)^2 \cos(\omega_e\tau/2)\right] \sin(\omega_A\tau) - \left(\frac{\omega_B}{\omega_e}\right) \sin(\omega_e\tau/2) \cos(\omega_A\tau) \tag{16}$$

ignoring relaxation. In Figure 3 examples of $g(\tau)$ are displayed for three different spin-pairs in 5CB. In order to take into account the spin−spin relaxation during the double-quantum preparation interval, eq 16 was multiplied with an exponential decay function corresponding to a line width of 40 Hz. The behavior of $g(\tau)$ is strongly dependent on D_{jk}. To obtain signals from all possible spin-pairs, it is usually necessary to perform experiments at a selection of τ values.

Table 3. Frequency Coordinates and Amplitudes of the Peaks in 2D Double-Quantum Spectroscopy of an Ensemble of Two-Spin Systems

observable coherence	freq coordinates (ω_1, ω_2)	amplitude
$\|4\rangle\langle 3\|$	$(\omega_\Sigma, {}^1/_2(\omega_\Sigma - \omega_e - 2\omega_A))$	$-(1 - \sin 2\theta)g(\tau)$
$\|2\rangle\langle 1\|$	$(\omega_\Sigma, {}^1/_2(\omega_\Sigma - \omega_e + 2\omega_A))$	$(1 + \sin 2\theta)g(\tau)$
$\|4\rangle\langle 2\|$	$(\omega_\Sigma, {}^1/_2(\omega_\Sigma + \omega_e - 2\omega_A))$	$-(1 + \sin 2\theta)g(\tau)$
$\|3\rangle\langle 1\|$	$(\omega_\Sigma, {}^1/_2(\omega_\Sigma + \omega_e + 2\omega_A))$	$(1 - \sin 2\theta)g(\tau)$

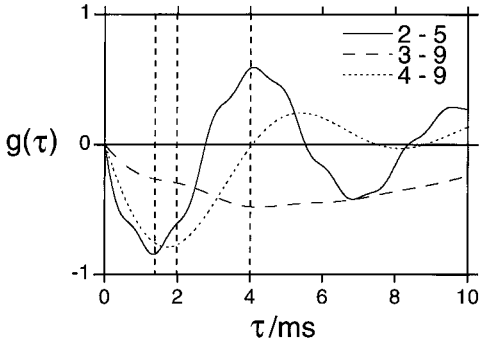

Figure 3. Simulated double-quantum excitation factors for three spin-pairs in 5CB as functions of the double-quantum preparation time. The following parameters were used: (2−5) $|\omega_\Delta/2\pi| = 1505$ Hz, $D_{jk}/2\pi = -183$ Hz, and $J_{jk}^{iso} = 11$ Hz; (3−9) $|\omega_\Delta/2\pi| = 610$ Hz, $D_{jk}/2\pi = -34$ Hz, and $J_{jk}^{iso} = 0$; (4−9) $|\omega_\Delta/2\pi| = 92$ Hz, $D_{jk}/2\pi = -87$ Hz, and $J_{jk}^{iso} = 7$ Hz. The three vertical lines indicate the experimental τ values used in this work.

3. Experimental Section

The sample of 5CB was purchased from Merck and used without further purification. The NMR experiments were performed at a field of 4.7 T on a Bruker MSL200 spectrometer using a standard 10-mm

(19) Solomon, I. *Phys. Rev.* **1955**, *99*, 559−565.

(20) Ernst, R. R.; Bodenhausen, G.; Wokaun, A. *Principles of Nuclear Magnetic Resonance in One and Two Dimensions*; Clarendon Press: Oxford, 1987.

(21) Kay, L. E.; McClung, R. E. D. *J. Magn. Reson.* **1988**, *77*, 258−273.

(22) Nakai, T.; McDowell, C. A. *Mol. Phys.* **1993**, *79*, 965−983.

high-resolution probe. The volume of the sample was approximately 1.5 mL. Two-dimensional ^{13}C NMR spectra were obtained by the pulse sequence described in the previous section. A modulated proton decoupling rf field was applied throughout the experiment. The decoupler field was switched between phases $\{0,\pi/2,\pi,3\pi/2\}$ every 1.5 ms. The decoupler frequency was set to the center of the ^1H spectrum in the isotropic liquid phase, and the decoupler field strength corresponded to a nutation frequency $|\omega_{1I}/2\pi| = 10.2$ kHz. Due to the rf heating problem in liquid crystals,[23] we reduced the decoupler power as much as possible while maintaining reasonable resolution. The modulated decoupling scheme described above was slightly superior to unmodulated decoupling. The four-step sequence provided adequate decoupling of all ring carbons, but the nitrile and the aliphatic carbons were still only poorly resolved. As a result, we only obtained accurate DD couplings within the biphenyl fragment. The ^{13}C peak assignment of 5CB was taken from the literature.[23]

The 2D data sets, 256 × 1024 points, were zero-filled to 1024 × 8192 points prior to Fourier transformation. For each t_1 value, between 256 and 384 transients were recorded which resulted in total acquisition times of 55−83 h. Reported dipole−dipole couplings are average values obtained from three double-quantum experiments with τ equal to 1.4, 2.0, and 4.0 ms as indicated in Figure 3. The temperature calibration was performed by letting the double-quantum pulse sequence run for 25 mins on an identical sample of 5CB with a capillary of ethylene glycol placed in the center. The chemical shift difference of ethylene glycol was then measured.[24] This procedure yielded a steady-state temperature of 28 ± 1 °C.

To suppress signals from isolated ^{13}C spins, and to produce pure absorption 2D peaks from the ^{13}C spin-pairs, we used an extensive phase cycle of the four rf pulses, the receiver reference phase, and the hardware phase shift of the digitized signals. The phase cycle was designed to pass signals from all desirable coherence transfer pathways $0 \rightarrow (\pm1) \rightarrow (\mp1) \rightarrow (-2) \rightarrow (-1)$ and $0 \rightarrow (\pm1) \rightarrow (\mp1) \rightarrow (+2) \rightarrow (-1)$. The phase cycle was specified as follows:

$$\phi_1 = \phi_1^0 + \pi \,\mathrm{floor}(m_2/4) \tag{17}$$

$$\phi_2 = \phi_2^0 + (\pi/2)\,\mathrm{floor}(m_2/8) \tag{18}$$

$$\phi_3 = \phi_3^0 \tag{19}$$

$$\phi_4 = (\pi/2)m_2 \tag{20}$$

$$\phi_1^0 = \phi_2^0 = \phi_3^0 = (\pi/4)m_1 \tag{21}$$

$$\phi_{\mathrm{data}} = (\pi/2)\,\mathrm{floor}(m_2/32) \tag{22}$$

where the transient counter is $m_2 = 0, 1, 2, ..., 127$ and the t_1 increment counter is $m_1 = 0, 1, 2, ..., 255$. The function floor(x) indicates the largest integer not greater than x. The receiver phase was adjusted on each acquired transient so as to conform to the equation

$$\phi_1 - 2\phi_2 - \phi_3 + \phi_4 + \phi_{\mathrm{rec}} + \phi_{\mathrm{data}} = \phi_1^0 - 2\phi_2^0 - \phi_3^0 \tag{23}$$

In these equations, the four rf pulses have phases ϕ_1, ϕ_2, ϕ_3, and ϕ_4, and the quadrature receiver uses a reference phase ϕ_{rec} during signal detection. All these phases refer to the rotating-frame fields and are opposite in sign to the phase shifts of the electronic carrier wave.[18] The digitized NMR signals are added together after multiplying by the complex factor $\exp(i\phi_{\mathrm{data}})$. The t_1-incrementation of the phases of the first three pulses in steps of $\pi/4$ discriminates the frequencies of the (±2)Q coherences:[9] Under suitable symmetry conditions (see Appendix), pure absorption 2D spectra are obtained after a cosine Fourier transform in the t_1 dimension.[20] In practice, tables for the phases were precalculated using a Mathematica routine[25] and then inserted into the pulse programmer code.

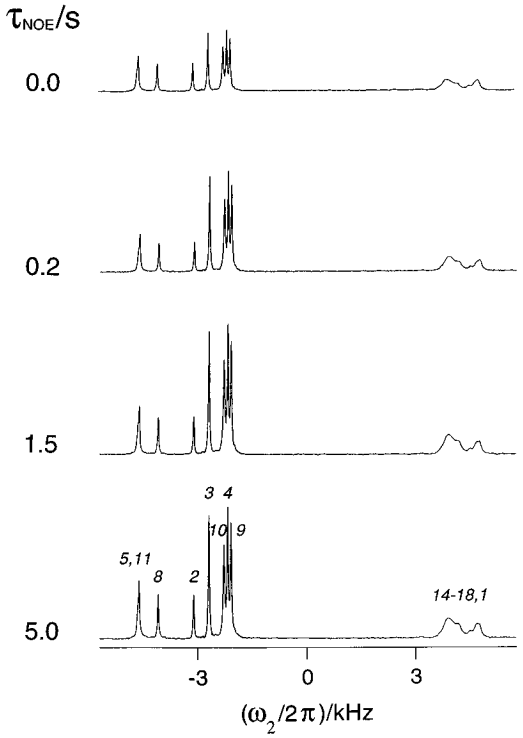

Figure 4. One-pulse ^{13}C spectra of 5CB with various durations of the ^1H pre-irradiation field. The experimental temperature was 28 ± 1 °C, and 32 transients were recorded for each spectrum. The sense of the frequency is conventional: The axis labeling employs careful considerations of the signs of the interactions (see text).

Since the NMR signal from the naturally occurring ^{13}C spin-pairs is extremely weak, we established a nuclear Overhauser enhancement (NOE) of the ^{13}C magnetization by means of 3.0-s unmodulated low-intensity ^1H irradiation prior to each ^{13}C pulse sequence.[19] The effect of this spectral enhancement in a simple one-pulse ^{13}C experiment is depicted in Figure 4. The ^1H pre-irradiation typically enhances the ^{13}C signal by a factor of 2. The build-up rates of the signals are functions of the ^{13}C spin−lattice relaxation times.[26] The peaks from the protonated ring carbons (with $T_1 \approx 0.2$ s) are substantially enhanced after only 0.2 s, whereas signals coming from nonprotonated ring carbons (with $T_1 \approx 1.4$ s) require much longer ^1H irradiation. The proton rf field strength used to establish NOE-enhanced ^{13}C magnetization corresponded to a nutation frequency $|\omega_{1I}/2\pi| = 0.6$ kHz.

4. Estimation of the Dipolar Couplings

A typical two-dimensional 2Q spectrum is shown in Figure 5. This shows only the spectral region corresponding to the ring core carbons. Due to the high mobility and the presence of extensive $^1H-^1H$ couplings, the ^{13}C dipole−dipole couplings in the aliphatic chain are poorly resolved and are not shown.

The 2D spectrum exhibits signals from three classes of spin systems. **First case:** If the two ^{13}C's are at sites with identical chemical shifts, an A_2 spectrum is obtained. This gives rise to an antiphase doublet with a splitting equal to $3|D_{jk}|$. **Second case:** When $|\omega_\Delta| \gg |\omega_B|$ (an AX system), two antiphase doublets appear in the spectrum with a splitting of $2|\omega_A|$. In this case, extraction of D_{jk} requires prior knowledge of the isotropic J-coupling. Reasonable values of J_{jk}^{iso} were obtained by comparing the cyanobiphenyl moiety with similar compounds with known scalar couplings.[27,28] **Third case:** If $|\omega_\Delta|$ is of the same order of magnitude as $|\omega_B|$ one obtains an AB spectrum,

(23) Fung, B. M. *J. Magn. Reson.* **1990**, *86*, 160−163.
(24) Ammann, C.; Meier, P.; Merbach, A. E. *J. Magn. Reson.* **1982**, *46*, 319−321.
(25) Wolfram, S. *Mathematica: A System for Doing Mathematics by Computer*; Addison-Wesley: Reading, 1988.
(26) Kuhlmann, K. F.; Grant, D. M. *J. Chem. Phys.* **1971**, *55*, 2998−3007.
(27) Wray, V. *Prog. NMR Spectrosc.* **1979**, *13*, 177−256.
(28) Krivdin, L. B.; Della, E. W. *Prog. NMR Spectrosc.* **1991**, *23*, 301−610.

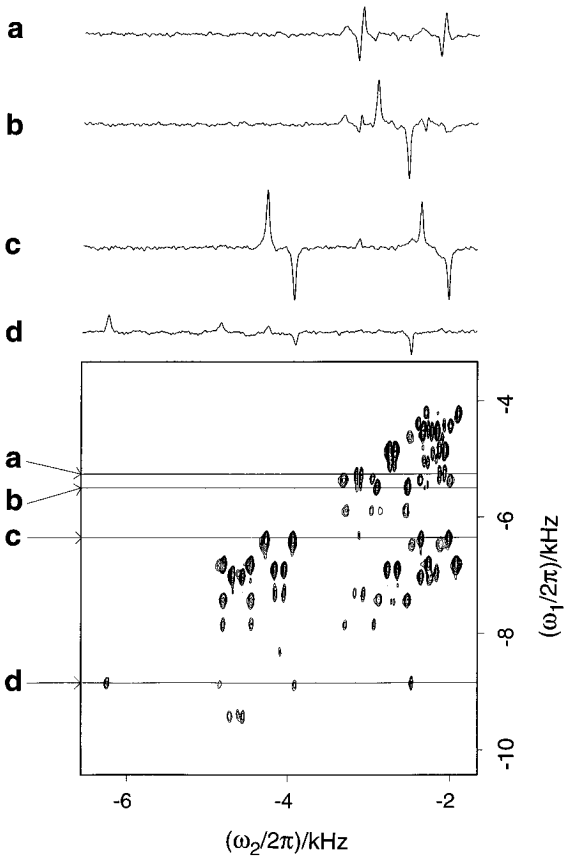

Figure 5. Part of a 2D ^{13}C spectrum of 5CB obtained by the pulse sequence described in the text. The double-quantum preparation period was $\tau = 4.0$ ms. In a−d we show slices along the ω_2 axis, corresponding to the following spin-pairs: (a) 2−9; (b) 3−7; (c) 4−8; (d) 5−8 (outer doublet) and 8−11 (inner doublet). The sense of the frequency axes is conventional (see caption of Figure 4).

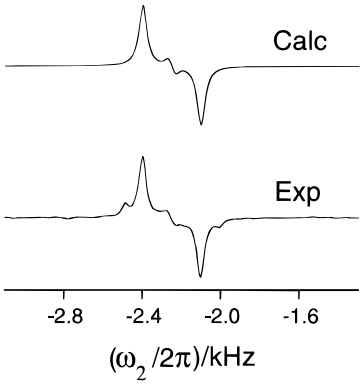

Figure 6. Experimental and calculated subspectra from spins at sites 4 and 9. The double-quantum preparation period was $\tau = 1.4$ ms.

which may be analyzed to yield separate values of D_{jk} and J_{jk}^{iso} if the sign of one of the two couplings is known. This is the case for the coupling between sites 4 and 9. In Figure 6 we show a slice along the ω_2 axis containing the subspectrum from carbons 4−9. From line shape simulations using the expressions in Table 3, $D_{4-9}/2\pi$ and J_{4-9}^{iso} were found to be −87 and 7 Hz, respectively. The calculated spectrum is included in Figure 6. The small extra peaks in the experimental line shape are due to a partial overlap in the ω_1 dimension from signals produced by the spin-pairs 4−6 and 9−13.

5. Interpretation of the Dipolar Couplings

It is far from trivial to interpret experimental dipole−dipole couplings in a flexible molecule like 5CB. In general, it is not possible to describe the molecular order by a single ordering matrix. The orientational order parameters are functions of the internal motion. Different strategies have been proposed to deal with this problem. One model is based on the approximation that the molecules only adopt a small number of minimum-energy conformations. This is called the rotational isomeric state (RIS) approximation. More realistic approaches allow for continuous bond rotations and the influence of the molecular conformation on the order parameters.

In the following discussion, we analyze the obtained dipolar couplings in various ways, in order to assess the ability of our method to discriminate between various motional and ordering models, and to estimate its accuracy and its reliability in a system which is already well understood.

5.1. Orientational Order of the Aromatic Rings. The analysis of the experimental data is considerably simplified if we concentrate on rigid fragments of the molecule. Consider for example the phenyl rings in the 5CB molecule. The ring connected to the CN group will be denoted by R1, while the ring linked to the aliphatic chain will be called R2. Two separate local axis systems may be attached to the aromatic rings, with the *z* axes in the direction of the *para* axes, and the *y* axes normal to the ring planes. As discussed by Emsley et al.,[11,12] the local Saupe ordering matrices for the two rigid fragments, $\mathbf{S}^{R1}$ and $\mathbf{S}^{R2}$, are diagonal in these frames provided that internal motion generates an effective C_{2v} symmetry. The dipolar couplings can in this case be expressed as[12]

$$D_{jk} = -\frac{\mu_0}{4\pi}\frac{\gamma_C^2\hbar}{r_{jk}^3}\left[S_{zz}^{R}\frac{1}{2}(3\cos^2\theta_{jk}^{z} - 1) + (S_{xx}^{R} - S_{yy}^{R})\frac{1}{2}(\cos^2\theta_{jk}^{x} - \cos^2\theta_{jk}^{y})\right] \quad (24)$$

where $S_{\alpha\alpha}^{R}$ ($\alpha = x, y, z$) are principal values of the local ordering matrices, and θ_{jk}^{α} are angles between the spin−spin vector and the ring-fixed principal axes. By fitting the DD couplings to the above equation we obtained the following result: $S_{zz}^{R1} = S_{zz}^{R2} = 0.52$, $S_{xx}^{R1} - S_{yy}^{R1} = 0.05$, and $S_{xx}^{R2} - S_{yy}^{R2} = 0.04$. Anisotropic *J*-couplings were ignored and hexagonal ring symmetry was assumed. The distance between two neighboring ^{13}C spins in the aromatic moieties was taken to be $r_{CC} = 1.40$ Å, which is the appropriate value for an undistorted benzene ring.[29]

A complete analysis would in principle require averaging over vibrational motion. For ^{1}H−^{1}H dipolar couplings, it has been shown that vibrational corrections are significant.[11] Due to the more rigid carbon skeleton, this is not so important for ^{13}C−^{13}C couplings; Diehl et al.[30] have shown that the vibrational contributions to the DD couplings in benzene are less than 1%. We neglected the vibrational displacements of the carbon nuclei in our calculations.

5.2. Jump Motions of the Biphenyl Fragment. The analysis in the previous section yielded a set of local order parameters reflecting the orientational order of the two individual rings with respect to the external field. However, these parameters do not reveal the orientation distribution of the two rings with respect to each other. Such information can only be obtained from the inter-ring DD couplings. Furthermore, the couplings must be interpreted using models for the distribution of torsional angles between the two rings.

(29) Laaksonen, A.; Wang, J.; Boyd, R. J. *Chem. Phys. Lett.* **1995**, *241*, 380−386.
(30) Diehl, P.; Bösiger, H.; Jokisaari, J. *Org. Magn. Reson.* **1979**, *12*, 282−283.

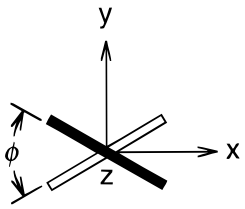

Figure 7. Molecular-fixed frame used to analyze the $^{13}C-^{13}C$ dipolar couplings within the biphenyl fragment of 5CB.

To extract the ordering and structure of the biphenyl core we make some assumptions about the symmetry of this fragment, and about the nature of the internal degrees of freedom. The simplest possible model for the internal motion is to assume that the two phenyl rings jump between a small number of conformations, and that the probabilities of the different conformations are independent of the overall orientation of the molecule with respect to the nematic director. We further assume that (i) there are no geometrical or motional differences between the two rings, (ii) only four equally populated structures exist ($\phi = \pm\phi_m$ and $\pi \pm \phi_m$, cf. Figure 7), and (iii) the jumps between the four equivalent conformations are fast compared to D_{jk}^{-1}. Given these assumptions, the best choice for a molecular-fixed frame is shown in Figure 7; the *z* axis coincides with the biphenyl *para* axis, and the *x* axis is fixed in the plane bisecting the ring planes. Sinton et al.[13] have shown that the local ordering tensor describing the biphenyl core is diagonal in this frame. Since all four conformations have the same shape, they have identical ordering matrices.

All dipolar couplings (regardless of their experimental accuracy) were fitted to eq 24. The fitting program, which is based on a Monte Carlo subroutine,[31] minimizes the weighted sum square error

$$\text{error} = \sum_{j<k} \frac{[D_{jk}^{\text{expr}} - D_{jk}^{\text{calc}}]^2}{[D_{jk}^{\text{expr}}]^2} \qquad (25)$$

where D_{jk}^{expr} and D_{jk}^{calc} are the experimental and calculated couplings, respectively. As before, *J*-anisotropy was ignored, the phenyl rings were assumed to have perfect hexagonal symmetry ($r_{CC} = 1.40$ Å), and the following standard bond lengths were used: $r_{1-2} = 1.43$ Å and $r_{5-8} = 1.49$ Å. This analysis resulted in the following parameters: $S_{zz} = 0.53$, $S_{xx} - S_{yy} = 0.06$, and $\phi_m = 36°$. The torsional angle agrees fairly well with previous studies of 5CB in which the RIS model was adopted. For example, Sinton et al.[13] obtained a value of $\phi_m = 29-32°$ depending on the assumed symmetry of the biphenyl fragment. The orientational ordering also agrees with other investigations.[12,15] Rather large relative errors were observed for some of the D_{jk} values (Table 4). The discrepancy between D_{jk}^{expr} and D_{jk}^{calc} probably stems from a combination of *J*-anisotropy, limited experimental accuracy, and geometrical ring distortions. The fact that good agreement with previous analyses is obtained, despite discrepancies in some individual dipolar couplings, is an indication that the method as a whole is not very sensitive to assumptions such as neglect of *J*-anisotropy.

In order to study the effect of bond lengths on the calculated parameters we repeated the fitting procedure with two $^{13}C-^{13}C$ distances kept fixed, while the third was allowed to vary. The r_{5-8} bond length was chosen to be the variable one, since this distance has the greatest influence on the estimate of ϕ_m. The result is shown in Table 5. The order parameters are clearly rather insensitive to changes in r_{5-8}. However, the torsional angle shows some variation for different inter-ring distances. The fitting error exhibits a weak minimum at $r_{5-8} = 1.49$ Å.

(31) Chandler, J. P. Program No. 307, 1982, QCPE, Chemistry Department, Indiana University, Bloomington, IN 47405.

Table 4. Experimental and Calculated ^{13}C Dipolar Couplings for 5CB Adopting the RIS Model

carbons	$D_{jk}^{\text{expr}}/2\pi$ (Hz)	$D_{jk}^{\text{calc}}/2\pi$ (Hz)
1−3,7	−175	−176
1−4,6	−67	−66
1−5	−57	−53
2−3,7	126	133
2−4,6	−177	−180
2−5	−183	−184
2−8	−54	−51
2−9,13	−27	−27
3−4,6−7	−1444	−1469
5−3,7	−174	−180
3−7	127	128
8−3,7	−63	−63
3,7−9,13	−34	−35
3,7−10,12	−19	−17
4−6	130	128
8−4,6	−169	−169
4,6−9,13	−87	−86
4,6−10,12	−34	−35
5−8	−1224	−1219
5−9,13[a]	−170	−169
5−10,12	−63	−63
5−11	−50	−51
8−10,12	−177	−180
8−11	−181	−184
9−10,12−13	−1415	−1469
9−13	131	128
11−10,12	139	133
10−12	132	128
fitting error:[b]	0.024	

[a] Assignment uncertain, could also be 11−9,13. [b] Defined as in Table 5.

Table 5. Fitted Order Parameters and Torsional Angles as a Function of r_{5-8} Adopting the RIS Model

r_{5-8} (Å)	S_{zz}	$S_{xx} - S_{yy}$	ϕ_m (deg)	fitting error[a]
1.46	0.53	0.06	38	0.026
1.47	0.53	0.06	37	0.025
1.48	0.53	0.06	36	0.024
1.49	0.53	0.06	36	0.024
1.50	0.53	0.06	35	0.025
1.51	0.53	0.06	34	0.027
1.52	0.54	0.06	33	0.028

[a] Defined as follows: $N^{-1}\sum_{j<k}|D_{jk}^{\text{expr}} - D_{jk}^{\text{calc}}|/|D_{jk}^{\text{expr}}|$, where N is the number of dipole−dipole couplings.

5.3. A Continuous Distribution of Inter-ring Angles. A more realistic model than the RIS approximation allows a continuous distribution of torsional angles and attempts to take into account the dependence of the overall molecular orientation distribution on the molecular shape, as defined by the conformational angle ϕ. The motionally averaged dipolar couplings can in this model be expressed as

$$D_{jk} = \int D_{jk}(\phi) p(\phi)\, \mathrm{d}\phi \qquad (26)$$

where $p(\phi)$ is the probability distribution for the angle of twist. The conformation-dependent DD couplings $D_{jk}(\phi)$ are still given by eq 24 if one remembers that r_{jk}, $S_{\alpha\alpha}$, and θ_{jk}^{α} now all are continuous functions of ϕ. As usual, we assume that a large separation of time scales allows independent averaging of internal and overall degrees of freedom.

We estimated $p(\phi)$ using a version of the additive potential (AP) model introduced by Emsley, Luckhurst, and Stockley[32] and referred to as the ELS model. A mean potential $U(\beta_{DM}, \gamma_{DM}, \phi)$ is derived and expressed as a superposition of two terms

$$U(\beta_{DM}, \gamma_{DM}, \phi) = U_{\text{ext}}(\beta_{DM}, \gamma_{DM}, \phi) + U_{\text{int}}(\phi) \quad (27)$$

where $U_{\text{ext}}(\beta_{DM}, \gamma_{DM}, \phi)$ is the potential of mean torque. Here β_{DM} and γ_{DM} are Euler angles relating the orientation of the director frame D to the molecular-fixed axis system M. The third angle α_{DM} is irrelevant for uniaxial mesophases. For a flexible molecule like 5CB, $U_{\text{ext}}(\beta_{DM}, \gamma_{DM}, \phi)$ depends on both orientation and conformation. As above, the molecular frame M is chosen with the z axis in the direction of the *para* axis and the x axis in the plane bisecting the two phenyl ring planes. The second term in eq 27 is a mean conformational potential which depends only on ϕ.

The second-rank truncated potential of mean torque is written as

$$U_{\text{ext}}(\beta_{DM}, \gamma_{DM}, \phi) = -\epsilon_{20}(\phi)C_{20}(\beta_{DM}, \gamma_{DM}) - \epsilon_{22}(\phi)2\text{Re}C_{22}(\beta_{DM}, \gamma_{DM}) \quad (28)$$

where $C_{2m}(\beta_{DM}, \gamma_{DM})$ are modified spherical harmonics.[33] The interaction parameters $\epsilon_{2m}(\phi)$ define the ordering potential imposed from the anisotropic environment; it is assumed that each rigid subunit l in the molecule makes its own contribution to $\epsilon_{2m}(\phi)$

$$\epsilon_{2m}(\phi) = \sum_l \sum_p \epsilon_{2p}^l D_{pm}^2(\Omega_l) \quad (29)$$

where $D_{pm}^2(\Omega_l)$ are elements of the second-rank Wigner rotation matrix, and Ω_l is a set of Euler angles specifying the orientation of the lth segment with respect to the molecular-fixed frame. Since the two rings have a common z axis and from our assumption that no geometrical or motional differences exist between the two aromatic moieties, two interaction coefficients, ϵ_{20}^{R} and ϵ_{22}^{R}, are sufficient to define the second-rank potential of mean torque.

We used the following expression for the periodic inter-ring potential

$$U_{\text{int}}(\phi) = U_2 \cos 2\phi + U_4 \cos 4\phi \quad (30)$$

where U_2 and U_4 are expansion coefficients.

The distribution function for the torsional angle and the mean potential are related to each other by

$$p(\phi) = Z^{-1} \int\int \exp[-U(\beta_{DM}, \gamma_{DM}, \phi)/RT] \times \sin\beta_{DM}\, \mathrm{d}\beta_{DM}\, \mathrm{d}\gamma_{DM} \quad (31)$$

where Z is the orientational partition function, defined so that $p(\phi)$ is normalized to unity over all orientations.

Thus, in this mean-field approach there are four free parameters: ϵ_{20}^{R}, ϵ_{22}^{R}, U_2, and U_4. Unfortunately, only one $^{13}\text{C}-^{13}\text{C}$ dipolar coupling (D_{4-9}) is reasonably sensitive to the torsional angle, so that only the ratio between U_2 and U_4 could be determined. This ratio is in principle sufficient to locate the minimum of the inter-ring potential in eq 30, but the height of the potential barrier cannot be obtained from the data set. In practice, we kept U_2 fixed and varied the other three adjustable parameters until a minimum in the target function eq 25 was found. The fitting procedure was repeated for many different values of U_2. The results are given in Table 6. When U_2 is less than -1 kJ mol^{-1}, the fitting error is constant and the calculated couplings are virtually identical to those found using the RIS approximation in the previous section (cf. Table 4). So, on the basis of fitting error we cannot discriminate between the discrete jump and continuous distribution models.

Table 6. Fitting Parameters Assuming a Continuous Distribution of Torsional Angles in 5CB

U_2[a] (kJ mol^{-1})	U_4 (kJ mol^{-1})	ϵ_{20}^{R} (kJ mol^{-1})	ϵ_{22}^{R} (kJ mol^{-1})	ϕ_m[b] (deg)	fitting error[c]
−20.0	16.5	3.17	0.59	36	0.024
−15.0	12.7	3.17	0.59	36	0.024
−10.0	8.8	3.17	0.60	37	0.024
−8.0	7.3	3.17	0.60	37	0.024
−6.0	5.6	3.17	0.60	37	0.024
−5.0	4.7	3.17	0.60	37	0.024
−4.0	3.7	3.17	0.60	37	0.024
−3.0	2.6	3.17	0.60	37	0.024
−2.0	1.1	3.17	0.60	31	0.024
−1.0	−2.5	3.17	0.61	0	0.024

[a] Kept fixed. [b] Minimum in the torsional potential. [c] Defined as follows: $N^{-1}\sum_{j<k}|D_{jk}^{\text{expr}} - D_{jk}^{\text{calc}}|/|D_{jk}^{\text{expr}}|$, where N is the number of dipole−dipole couplings.

A striking feature in Table 6 is the insensitivity of the interaction parameters ϵ_{20}^{R} and ϵ_{22}^{R} to the shape of the inter-ring potential. This means that the conformation-dependent local order parameters of the biphenyl fragment are well-defined since they are completely determined by the potential of mean torque[34]

$$S_{zz}(\phi) = Q(\phi)^{-1} \int\int {}^1/_2(3\cos^2\beta_{DM} - 1) \times \exp[-U_{\text{ext}}(\beta_{DM}, \gamma_{DM}, \phi)/RT] \sin\beta_{DM}\, \mathrm{d}\beta_{DM}\, \mathrm{d}\gamma_{DM} \quad (32)$$

and

$$S_{xx}(\phi) - S_{yy}(\phi) = Q(\phi)^{-1} \int\int {}^3/_2 \sin^2\beta_{DM} \cos 2\gamma_{DM} \times \exp[-U_{\text{ext}}(\beta_{DM}, \gamma_{DM}, \phi)/RT] \sin\beta_{DM}\, \mathrm{d}\beta_{DM}\, \mathrm{d}\gamma_{DM} \quad (33)$$

where the ϕ-dependent orientational partition function $Q(\phi)$ is given by

$$Q(\phi) = \int\int \exp[-U_{\text{ext}}(\beta_{DM}, \gamma_{DM}, \phi)/RT] \times \sin\beta_{DM}\, \mathrm{d}\beta_{DM}\, \mathrm{d}\gamma_{DM} \quad (34)$$

The local order parameters are depicted in Figure 8. Note the dependence of the biaxiality parameter $S_{xx}(\phi) - S_{yy}(\phi)$ on the conformation of the biphenyl fragment. The RIS analysis resulted in a torsional angle of $\phi_m \approx 36°$, and at this angle Figure 8 predicts values of 0.53 and 0.06 for S_{zz} and $S_{xx} - S_{yy}$, respectively. These parameters fully agree with the values found in section 5.2.

We close this section by discussing the probability distribution $p(\phi)$ for the angle of twist. When a value of U_2 less than -3 kJ mol^{-1} is used, the best determination of U_4 leads to a minimum in $U_{\text{int}}(\phi)$ at $\approx 36°$, i.e. the same value found assuming a jump motion of the phenyl rings. This almost exactly coincides with results from a previous AP analysis of ^{1}H dipolar couplings in 5CB-d_{11}.[16] However, when U_2 is increased to -2.0 kJ mol^{-1}, our mean-field calculation results in a minimum in the inter-ring potential at 31°. For $U_2 = -1.0$ kJ mol^{-1}

(32) Emsley, J. W.; Luckhurst, G. R.; Stockley, C. P. *Proc. R. Soc. London A* **1982**, *381*, 117−138.

(33) Brink, D. M.; Satchler, G. R. *Angular momentum*; Clarendon Press: Oxford, 1993.

(34) Celebre, G.; Longeri, M.; Emsley, J. W. *J. Chem. Soc., Faraday Trans. 2* **1988**, *84*, 1041−1052.

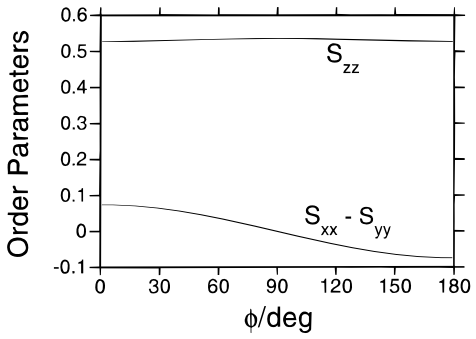

Figure 8. Conformation-dependent local order parameters for the biphenyl fragment in 5CB, estimated by an ELS analysis of the experimental $^{13}C-^{13}C$ dipolar couplings. The change in sign of $S_{xx} - S_{yy}$ for $\phi > 90°$ is associated with a change in molecular shape as the dihedral angle increases, as is apparent from Figure 7.

(indicating a low rotational barrier) the fitting actually predicts a flat molecule ($\phi_m = 0°$) as the most probable conformation. The quality of the fit is about the same for all the above calculations. The conclusion of these findings is that our ^{13}C data set is not sensitive enough to extract an unambiguous distribution of torsional angles, without making some assumptions about the form of the torsional potential. However, once a physically reasonable barrier height is inserted into the fitting procedure, the calculation does converge to a torsional angle estimate in agreement with previous data.

6. Conclusions

The conclusions of our study may be summarized as follows;

(i) In a system like 5CB, which orients essentially perfectly and homogeneously along the external field, the double-quantum ^{13}C technique is a convenient and simple method of obtaining a large number of informative dipolar couplings between ^{13}C spins in the core region of the molecule. Most of the couplings are easily and unambiguously assigned.

(ii) The method does not require isotopic labeling, and can in principle be applied to systems of arbitrary size, within limitations of sensitivity.

(iii) The signal acquisition times are typically much longer than for competing methods such as multiple-quantum ^1H NMR. However, the extraction of dipolar couplings from the experimental spectrum is much easier, and free from ambiguity except in exceptional situations of accidental degeneracy.

(iv) The method is less promising for aliphatic chains, where molecular motion and strong $^1H-^1H$ couplings typically make it difficult to obtain a well-decoupled and well-resolved ^{13}C NMR spectrum.

(v) The large $^{13}C-^{13}C$ couplings within the aromatic core region are readily interpreted in terms of the orientational order parameters of the individual benzene rings. Interference from *J*-anisotropy does not seem to be a very serious problem.

(vi) In 5CB, the inter-ring $^{13}C-^{13}C$ dipolar couplings may be interpreted to yield information on the torsional angle distribution around the C−C bond connecting the rings. However, the relatively low sensitivity of these couplings to details of molecular conformation makes it difficult to develop a precise motional model from the ^{13}C spectrum alone. The mean-field analysis must be supplemented by assuming a reasonable form of the torsional potential. In that case, we obtain results in close agreement with measurements on isotopically-labeled material.

Acknowledgment. We would like to acknowledge useful discussions with A. Maliniak, K. T. Summanen, and S. C. Shekar. We would also like to thank J. Jokisaari for providing us with a manuscript prior to its publication and O. G. Johannessen for skilful technical assistance. This work was supported by the Swedish Natural Science Research Council.

Note Added in Proof. Recently, J. Kaski, J. Vaara, and J. Jokisaari performed a thorough theoretical and experimental study of $^{13}C-^{13}C$ dipolar couplings in oriented benzene (*J. Am. Chem. Soc.* In press). They found that the ratio $|J_{jk}^{aniso}/D_{jk}|$ is less than 2% for all three couplings in benzene, which supports our assumption that *J*-anisotropy does not cause serious problems in the analysis of the ^{13}C data set.

Appendix

Amplitudes and Phases in 2D Double-Quantum Spectroscopy of an AB System. It is far from obvious that the 2D spectral peaks in a 2Q spectrum of an AB system have exactly the same amplitudes as in the ordinary 1D spectrum (except for a sign change), or that the coherence transfers through (±2)Q coherences have sufficient symmetry that the pure absorption phase in the 2D spectrum is assured. The main theoretical work on the subject[21] did not explore the possibility of obtaining pure absorption 2D spectra, and only analyzed the case where the last pulse had a flip angle of $3\pi/4$. In this case, the (±2)Q pathways have very different amplitudes. Sensitivity is degraded and pure absorption 2D spectra are certainly not possible. The discussion below examines this issue in general terms which are also applicable to strongly-coupled systems of more than two spins.

Before examining the 2Q spectra in detail, it is worthwhile to look first at the conventional 1D spectrum. In this case, the initial density operator for the coupled spin system (before the exciting $\pi/2$ pulse) is proportional to

$$\sigma_0 = S_{jz} + S_{kz} \tag{A1}$$

omitting for simplicity the unimportant unity operator and the prefactor for nuclear Overhauser enhanced Zeeman magnetization. A $(\pi/2)_x$ pulse excites coherences $|r\rangle\langle s|$ according to

$$V_x\sigma_0V_x^\dagger = \sum_{rs}\langle r|V_x\sigma_0V_x^\dagger|s\rangle|r\rangle\langle s| \tag{A2}$$

where *r*,*s* are summed over the four Hamiltonian eigenstates in Table 1, and V_x is the propagator for a $(\pi/2)_x$ pulse:

$$V_x = \exp\left\{-i\frac{\pi}{2}(S_{jx} + S_{kx})\right\} \tag{A3}$$

$V_x^\dagger$ denotes the adjoint of V_x. Each coherence $|r\rangle\langle s|$ induces a signal proportional to its own amplitude $\langle r|V_x\sigma_0V_x^\dagger|s\rangle$ and the quadrature detection factor

$$Q_{rs} = 2i\langle s|S_{j+} + S_{k+}|r\rangle \tag{A4}$$

Now since

$$V_x\sigma_0V_x^\dagger = -S_{jy} - S_{ky} = \frac{1}{2i}(S_{j-} + S_{k-}) - \frac{1}{2i}(S_{j+} + S_{k+}) \tag{A5}$$

the peak amplitude generated by a single (−1)Q coherence in the ordinary 1D spectrum is equal to

$$a_{rs}^{1D} = 2i\langle s|S_{j+} + S_{k+}|r\rangle\frac{1}{2i}\langle r|S_{j-} + S_{k-}|s\rangle$$
$$= |\langle r|S_{j-} + S_{k-}|s\rangle|^2 \tag{A6}$$

in accordance with the formal equivalence of continuous-wave absorption spectroscopy and one-pulse Fourier spectroscopy.[20]

It proves worthwhile to set these equations in a different form. The initial Zeeman operator $\sigma_0 = S_{jz} + S_{kz}$ may be written as

$$\sigma_0 = |1\rangle\langle 1| - |4\rangle\langle 4| \tag{A7}$$

It follows that the amplitude for excitation of coherence $|r\rangle\langle s|$ by a single $(\pi/2)_x$ pulse is given by

$$\langle r|V_x\sigma_0 V_x^\dagger|s\rangle = \langle r|V_x|1\rangle\langle 1|V_x^{\ \dagger}|s\rangle - \langle r|V_x|4\rangle\langle 4|V_x^\dagger|s\rangle \tag{A8}$$

Additional symmetry is invoked by noting that a π_x pulse (two $(\pi/2)_x$ pulses in succession) exchanges the states $|1\rangle$ and $|4\rangle$ by flipping both spins

$$V_x V_x|4\rangle = -|1\rangle \tag{A9}$$

The negative sign in the above equation derives from the identities

$$\exp(-i\pi S_{jx}) = -2iS_{jx} = -i(S_{j+} + S_{j-}) \tag{A10}$$

and

$$\exp(-i\pi S_x) = (-i)^2(S_{j+} + S_{j-})(S_{k+} + S_{k-}) \tag{A11}$$

Equation A9 therefore leads to

$$V_x|4\rangle = -V_x^\dagger|1\rangle \tag{A12}$$

and hence

$$\langle 4|V_x^\dagger = -\langle 1|V_x \tag{A13}$$

Furthermore, the operators $V_x = \exp\{-i(\pi/2)S_x\}$ and $V_x^\dagger = \exp\{+i(\pi/2)S_x\}$ are related to each other by a π rotation about the z axis:

$$V_x^\dagger = \Pi_z V_x \Pi_z^\dagger \tag{A14}$$

where $\Pi_z = \exp(-i\pi S_z)$. It follows that

$$\langle r|V_x^\dagger|s\rangle = (-)^{M_r - M_s}\langle r|V_x|s\rangle \tag{A15}$$

where $M_r - M_s$ is the difference in z-angular momentum for the states $|r\rangle$ and $|s\rangle$:

$$(S_{jz} + S_{kz})|r\rangle = M_r|r\rangle \tag{A16}$$

Since only (-1)Q coherences are observable, eq A8 can be reduced to

$$\langle r|V_x\sigma_0 V_x^\dagger|s\rangle = 2\langle r|V_x|1\rangle\langle 1|V_x^\dagger|s\rangle \tag{A17}$$

In 2D double-quantum spectroscopy, coherences $|1\rangle\langle 4|$ and $|4\rangle\langle 1|$ are first excited by the initial three-pulse sequence of duration τ. The density operator at the beginning of the evolution period is

$$U\sigma_0 U^\dagger = \langle 1|U\sigma_0 U^\dagger|4\rangle|1\rangle\langle 4| + \langle 4|U\sigma_0 U^\dagger|1\rangle|4\rangle\langle 1| + ... \tag{A18}$$

where U is the excitation propagator. The calculations of Nakai and McDowell[22] lead to the following explicit expressions for the excitation amplitudes:

$$\langle 1|U\sigma_0 U^\dagger|4\rangle = -ig(\tau) \tag{A19}$$

$$\langle 4|U\sigma_0 U^\dagger|1\rangle = +ig(\tau) \tag{A20}$$

where $g(\tau)$ is defined in eq 16. The amplitudes of the peaks in the 2D spectrum are governed by the amplitudes of the transfer process from the (± 2)Q coherences $|1\rangle\langle 4|$ and $|4\rangle\langle 1|$ to the four observable (-1)Q coherences.

Conversion of $|1\rangle\langle 4|$ coherence into $|r\rangle\langle s|$ coherence by a $(\pi/2)_x$ pulse may be written as

$$\begin{aligned}\langle r|V_x|1\rangle\langle 4|V_x^\dagger|s\rangle &= -\langle r|V_x|1\rangle\langle 1|V_x|s\rangle \\ &= (-)^{M_s}\langle r|V_x|1\rangle\langle 1|V_x^\dagger|s\rangle\end{aligned} \tag{A21}$$

where M_s is the z-angular momentum of state $|s\rangle$. Similarly, the amplitude for the conversion of $|4\rangle\langle 1|$ coherence into $|r\rangle\langle s|$ coherence by a $(\pi/2)_x$ pulse is

$$\begin{aligned}\langle r|V_x|4\rangle\langle 1|V_x^\dagger|s\rangle &= -\langle r|V_x^\dagger|1\rangle\langle 1|V_x^\dagger|s\rangle \\ &= (-)^{M_r}\langle r|V_x|1\rangle\langle 1|V_x^\dagger|s\rangle\end{aligned} \tag{A22}$$

where M_r is the z-angular momentum of state $|r\rangle$. It follows that the 2D peak amplitudes corresponding to $(+2)$QC in the t_1 dimension are given by

$$a_{rs}^{(+2)} = -{}^1/_2 ig(\tau)(-)^{M_s} a_{rs}^{1D} \tag{A23}$$

while the amplitudes of peaks corresponding to (-2)QC in the t_1 dimension are

$$a_{rs}^{(-2)} = +{}^1/_2 ig(\tau)(-)^{M_r} a_{rs}^{1D} \tag{A24}$$

Since for observable coherences $M_r = M_s - 1$, this corresponds to

$$a_{rs}^{(+2)} = a_{rs}^{(-2)} \tag{A25}$$

which shows that the $(+2)$Q and (-2)Q pathways have the correct balance and correct phase to ensure pure absorption 2D peaks after a cosine Fourier transform in the t_1 dimension. Equation A23 also shows that 2D peaks have exactly the same relative intensity as in the ordinary 1D spectrum but with a sign change for the peaks corresponding to observable coherences $|4\rangle\langle 2|$ and $|4\rangle\langle 3|$. This gives the characteristic "up−down−up−down" appearance. The complex factor i in eq A23 indicates that an additional $-\pi/2$ phase shift of the signal is necessary to achieve absorption phase.

It is also possible to derive these results by product operator calculations.[21,35] However, the arguments given here are based purely on symmetry considerations and may be extended to larger coupled spin systems. The properties of the (± 2)Q coherences and the observable (-1)QC's indicated above derive purely from the symmetries of the two extreme eigenstates $|1\rangle = |\alpha\alpha\rangle$ and $|4\rangle = |\beta\beta\rangle$. Identical properties apply to the extreme $(\pm N)$-quantum coherences in any system of N coupled spins-$^1/_2$, and those (-1)-quantum coherences which terminate on one of the extreme Zeeman eigenstates. It follows, for example, that 3-quantum spectroscopy of strongly-coupled three-spin systems yields pure absorption phase signals for those (-1)-quantum coherences which terminate on one of the extreme Zeeman eigenstates $|\alpha\alpha\alpha\rangle$ or $|\beta\beta\beta\rangle$, providing that a $\pi/2$ pulse is used for the $(\pm 3)\text{Q} \rightarrow (-1)$Q conversion. Furthermore, the amplitudes of those signals are the same as in the conventional 1D spectrum, apart from sign changes. Such symmetry properties are expected to be useful in multiple-quantum spectroscopy of strongly-coupled multiple-spin systems.

JA9601853

(35) Sørensen, O. W.; Eich, G. W.; Levitt, M. H.; Bodenhausen, G.; Ernst, R. R. *Prog. NMR Spectrosc.* **1983**, *16*, 163−192.